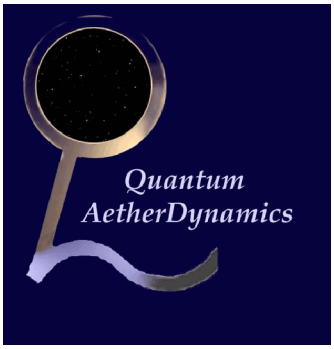

Quantum AetherDynamics Institute (QADI)

Collective Aether-Cell Coherence and the Neutron-to-Gravity Source Problem:

Geometric Bounds, Branch Selection, and Thermodynamic Completion

David W. Thomson III
Quantum AetherDynamics Institute (QADI), Alma, Illinois, USA
ORCID: 0000-0002-5830-5427
Existing work identifier: 10.5281/zenodo.22102013

Version 1.3 – October 18, 2026

This article is published by the Quantum AetherDynamics Institute (QADI).

It develops the Aether Physics Model (APM)

Abstract

We determine what a collective Aether-cell geometry can contribute to the neutron-to-gravity source problem before a microscopic interaction energy is known. A positive Fejér/Toeplitz kernel extends the prescribed single-unit deformation while preserving winding and an assumed two-seat organization. We retain its calculable density domains and prove the full-coherence asymptotic limit by dominated convergence. An explicit nearest-neighbor phase-chain distribution realizes the Toeplitz correlations without interpreting an inverse covariance matrix as a derived physical force law. The main result is a source-completion theorem. For conserved baryon density n_B, fixed neutron fraction Y_n, and a differentiable branch with $D_q \neq 0$, the geometric constraint implies $dq/d\ln n_B = \chi_M = -D/(3D_q)$. If a local, isotropic, constrained-equilibrium energy contribution is $m_e c^2 n_B u(\nu_B, Y_n, M, q)$, with $\nu_B = n_B \lambda_C^3$, its pressure is $m_e c^2 n_B(\nu_B u_{\nu_B} + \chi_M u_q)$. This gives a precise route from a future QMU interaction calculation to energy density, stress, and a spherical gravitational source. For a coherence-only energy, it also yields the branchwise composition identity $Y_n \partial\varepsilon_A/\partial Y_n = p_A$ at fixed baryon density. We prove that geometry and conductance identities alone cannot identify u, its gravitational normalization, or the preferred collective branch. At the first prescribed recruitment boundary, χ changes from 10.74768 to 0.87390; continuous-pressure matching consequently imposes a nontrivial energy-derivative condition in addition to geometric continuity. The construction thus supplies quantitative source constraints and a reproducible completion procedure, rather than a completed neutron-specific gravity law. Numerical density bounds remain conditional on the supplied neutron reference radius; stellar comparison states are compatibility examples, not observational validation.

Keywords: Quantum Measurement Units; Aether Physics Model; neutron-to-gravity source; collective Aether cells; Fejér kernel; phase coherence; constitutive energy; pressure; gravitational source; branch transitions

1 The source problem and the contribution of this paper

The revised Aether Metric Coordinates (AMC) construction distinguishes an exterior geometric correspondence from an unresolved microscopic source law Thomson [2026]. In particular, a neutron equivalent-cell coordinate is well defined,

$$D_{\text{cell}} = (n_n V_{n0})^{-1/3} = \frac{r_{\text{WS}}}{r_{n0}}, \qquad r_{\text{WS}} = \left(\frac{3}{4\pi n_n}\right)^{1/3}, \tag{1}$$

but assigning a material strain, interaction energy, or gravitational source to that coordinate requires additional physics. The single-unit deformation family examined in AMC cannot register all supplied comparison densities at its fixed reference radius. A collective family can extend the mathematical range, but extension alone does not establish the source response.

This paper addresses that distinction constructively. Its contribution is to derive the geometric response coefficient that enters a constrained constitutive pressure, state the associated energy and branch-matching requirements, and connect the resulting stress to gravitational source bookkeeping. It also proves why an interaction energy remains indispensable. The fluid thermodynamic and GR relations used for that connection are established results Brown [1993], Oppenheimer and Volkoff [1939]; the contribution here is their explicit application to the collective QMU constraint, its branch ambiguity, and its recruitment boundaries.

The scope is a local, zero-temperature, isotropic constitutive sector without resolved gradient or surface energies. The collective geometry and the two-seat organization are model assumptions.

Neither a neutron rest-mass formula nor a neutron-only universal coupling to gravity is derived. No observational mass–radius or photon-path fit is used to normalize the source. A completed APM theory would have to derive the missing interaction energy from its microscopic matter–Aether dynamics.

2 Prescribed geometry and its reference scale

The supplied reference values are

$$r_{n0} = 0.840077655903 \text{ fm}, \qquad V_{n0} = 2.483401334974 \text{ fm}^3 \simeq \frac{4\pi}{3} r_{n0}^3. \tag{2}$$

Their upstream geometric derivation and physical uncertainty are not supplied. They specify the archived numerical example, not an independently established neutron size. In native QMU coordinates, $\widehat{n}_n = n_n \lambda_C^3$ and $\widehat{r}_{n0} = r_{n0}/\lambda_C$ give

$$n_n V_{n0} = \frac{4\pi}{3} \widehat{n}_n \widehat{r}_{n0}^3. \tag{3}$$

Every density threshold below scales as r_{n0}^{-3}. The dimensionless geometric results can therefore be separated from this dimensional input.

The single-unit phase ansatz is

$$\phi_\eta(\theta) = 2\theta + \eta \sin 2\theta, \qquad \phi'_\eta = 2(1 + \eta \cos 2\theta). \tag{4}$$

Its normalized arc length is

$$D(\eta) = \frac{1}{L_0} \int_0^\pi \sqrt{1 + 4\sin^2\theta (1 + \eta\cos 2\theta)^2}\, d\theta, \quad L_0 = 5.270367163191261. \tag{5}$$

The non-reversing phase range is $0 \le \eta \le 1$. On that range D decreases from 1 to 0.822767275558. The full positive-η mathematical continuation has its unique minimum at $\eta \simeq 1.05088538$, with $D_{\min} = 0.822115465507$. AMC supplies the conditional domain analysis of this prescribed family Thomson [2026]. The global minimum is not a universal matter-density bound.

3 A positive collective family

Let M phase contributors have the correlation matrix

$$C_{ij} = q^{|i-j|}, \quad i, j = 0, \ldots, M-1, \quad 0 \le q \le 1. \tag{6}$$

The scalar q is a specified correlation coordinate, not yet a physical interaction strength. For $v_j = e^{ijx}$, pair counting gives

$$F_{M,q}(x) = \frac{v^\dagger C v}{M} = 1 + 2 \sum_{k=1}^{M-1} \left(1 - \frac{k}{M}\right) q^k \cos kx. \tag{7}$$

Positivity of C follows, for example, from the phase-chain realization in Sec. 4. Thus $F_{M,q} \geq 0$. The collective phase and deformation are defined by

$$\phi'_{M,q}(\theta) = 2F_{M,q}(2\theta), \tag{8}$$

$$D(M,q) = \frac{L(M,q)}{L_0}, \qquad L(M,q) = \int_0^\pi \sqrt{1 + 4\sin^2\theta F_{M,q}(2\theta)^2}\, d\theta. \tag{9}$$

The constant Fourier term fixes $\phi(\pi) - \phi(0) = 2\pi$, and positivity prevents phase reversal. At $M = 2$, $F_{2,q} = 1 + q\cos x$ and the single-unit ansatz is recovered exactly with $q = \eta$. At $q = 0$, all M have $D(M, 0) = 1$.

At full coherence,

$$F_{M,1}(x) = \frac{1}{M}\left|\sum_{j=0}^{M-1} e^{ijx}\right|^2, \tag{10}$$

the Fejér kernel. Its coefficients follow from $M - k$ contributor pairs at lag k once the equal-contributor construction has been chosen. Winding and positivity alone do not select this kernel uniquely. Likewise, $q^{|i-j|}$ is an adopted correlation model, not a consequence of QMU unit identities.

Preserving an assumed elementary two-seat cell restricts $M = 2K$. At $q = 1$,

$$F_{2K,1}(x) = F_{2,1}(x)F_{K,1}(2x). \tag{11}$$

This exact factorization supports an intact-cell interpretation within the construction. It does not derive an energy cost for adding a cell.

4 Explicit local phase-chain realization

An inverse correlation matrix alone does not establish a physical force law or, for an unspecified non-Gaussian joint distribution, its conditional interaction graph. Here a local phase model can instead be constructed explicitly. Let φ_0 be uniform on the circle and let independent increments $\Delta_j = \varphi_{j+1} - \varphi_j$ have density

$$p_\kappa(\Delta) = \frac{e^{\kappa\cos\Delta}}{2\pi I_0(\kappa)}, \qquad q = \frac{I_1(\kappa)}{I_0(\kappa)}, \quad \kappa \geq 0. \tag{12}$$

The joint distribution is the explicitly local open-chain law

$$p(\varphi_0, \ldots, \varphi_{M-1}) = \frac{1}{2\pi}\prod_{j=0}^{M-2} p_\kappa(\varphi_{j+1} - \varphi_j). \tag{13}$$

With $z_j = e^{i\varphi_j}$, symmetry gives $\langle e^{i\Delta}\rangle = q$. Independence then gives the exact realization

$$\boxed{\langle z_i z_j^*\rangle = q^{|i-j|}.} \tag{14}$$

This proves existence of a nearest-neighbor phase-chain model with the stated correlations, rather than inferring locality solely from a covariance inverse. Grouping adjacent sites into two-seat cells leaves both intra-cell and inter-cell nearest-neighbor links.

The same matrix has the exact quadratic form, for $0 \le q < 1$,

$$x^\dagger C^{-1} x = |x_0|^2 + \frac{1}{1-q^2} \sum_{j=0}^{M-2} |x_{j+1} - q x_j|^2, \tag{15}$$

which supplies a second local representation. These are mathematical realizations, not derived ligamen dynamics. In particular, κ, the information cost $\kappa q - \ln I_0(\kappa)$, and $s = -\ln q$ have no assigned mechanical energy scale here. An energy, temperature, or quantum-state law would be needed for that identification. The singular matrix at $q = 1$ describes perfect correlation; singularity itself does not require physical recruitment.

5 Density domains and the branch-selection assumption

The registration is the constitutive constraint

$$D(M, q) = D_{\text{cell}}. \tag{16}$$

On a differentiable decreasing segment of a fixed M branch, the density domain is

$$\frac{1}{V_{n0}} \le n_n \le \frac{1}{V_{n0} D(M,1)^3}, \tag{17}$$

when that branch decreases throughout $0 \le q \le 1$. Numerical derivative checks support this property on the finite branches tabulated here; no all-M monotonicity theorem is assumed in the source-completion result, which requires only a local segment with $D_q \neq 0$.

One possible recruitment prescription keeps the smallest available even M until $q = 1$, then enters $M + 2$ at

$$D(M + 2, q_{\text{entry}}) = D(M, 1). \tag{18}$$

This rule gives continuous D, and hence continuous equivalent-cell size. It is a branch-selection postulate. Continuity fixes an entry value after the old and new branches have been chosen; it does not establish when recruitment is energetically favored.

Table 1: Reproduced boundaries under the saturation-and-minimum-M prescription, conditional on Eq. (2). The labels indicate prescribed collective branches, not observed phase transitions.

M	q_{entry}	$D(M,1)$	$n_{n,\text{exit}}$ (fm^{-3})
2	0	0.822767276	0.722972969
4	0.501895639	0.714396250	1.104423379
6	0.783729689	0.675690890	1.305295676
8	0.874531421	0.655990388	1.426463493

The supplied SLY4 endpoint has $n_n = 1.067746871408$ fm^{-3} and $D_{\text{cell}} = 0.722484044913$. It is represented by several collective states:

$$(M, q) \simeq (4, 0.9090005644), \quad (6, 0.7539783086), \quad (8, 0.7078711094). \tag{19}$$

The recruitment prescription selects the first. Geometry alone does not. These are compatibility examples based on a supplied EOS-associated density, not independent measurements of M or q.

The original EOS tables, composition data, and stellar solver are absent, so this package does not establish the endpoint's stability, causality, or stellar realization.

An equilibrium branch would instead minimize the total energy over the admissible states,

$$\mathcal{A}(n_n) = \{(M, q) : M \in 2\mathbb{N},\ 0 \le q \le 1,\ D(M, q) = D_{\text{cell}}\}. \tag{20}$$

Whether the prescribed hierarchy agrees with that minimization is a physical question for the missing energy functional. Finite-size, gradient, and recruitment costs may also matter.

6 A rigorous asymptotic bound

The pointwise arc-length integrand is at least one, so $D \ge D_{\text{abs}} = \pi/L_0$. For any finite continuous nonzero-winding kernel in this family the inequality is strict. At full coherence,

$$F_{M,1}(2\theta) = \frac{\sin^2(M\theta)}{M \sin^2\theta}. \tag{21}$$

Using symmetry about $\pi/2$ and $y = M\theta$ gives

$$M[L(M, 1) - \pi] = 2 \int_0^{M\pi/2} \left[\sqrt{1 + \frac{4 \sin^4 y}{M^2 \sin^2(y/M)}} - 1 \right] dy. \tag{22}$$

Extend the integrand by zero beyond $M\pi/2$. For $0 < y \le M\pi/2$, $\sin(y/M) \ge 2y/(M\pi)$ and $\sqrt{1+a} - 1 \le a/2$ imply the integrable majorant

$$0 \le \sqrt{1 + \frac{4 \sin^4 y}{M^2 \sin^2(y/M)}} - 1 \le \frac{\pi^2}{2} \min(y^2, y^{-2}). \tag{23}$$

Dominated convergence therefore proves

$$I = \int_0^\infty \left[\sqrt{1 + 4 \sin^4 y/y^2} - 1 \right] dy, \tag{24}$$

$$D(M, 1) = D_{\text{abs}} + \frac{A}{M} + o(M^{-1}), \qquad A = \frac{2I}{L_0}. \tag{25}$$

The corrected numerical evaluation is

$$I \simeq 1.2684637643, \qquad A \simeq 0.4813568865. \tag{26}$$

Version 1.2's slightly different coefficient resulted from numerical evaluation of the improper integral; the limiting geometry and finite-M values are unchanged. The supplied script checks the integral using period-wise quadrature with an analytic tail and independently checks the approach using high-M arc lengths.

For the stated reference scale,

$$D_{\text{abs}} = 0.596086108674, \tag{27}$$

$$n_{n,\text{abs}} = \frac{1}{V_{n0} D_{\text{abs}}^3} = 1.901192474720\ \text{fm}^{-3}, \tag{28}$$

$$n_{n,\text{abs}} - n_{n,M} = \frac{B}{M} + o(M^{-1}), \qquad B = \frac{3 n_{n,\text{abs}} A}{D_{\text{abs}}}. \tag{29}$$

This is a supremum for the registered finite-cell geometry, not a derived upper density for physical neutron matter. No finite M attains the meridional limit. An actual stellar endpoint also depends on its total equation of state and phase structure.

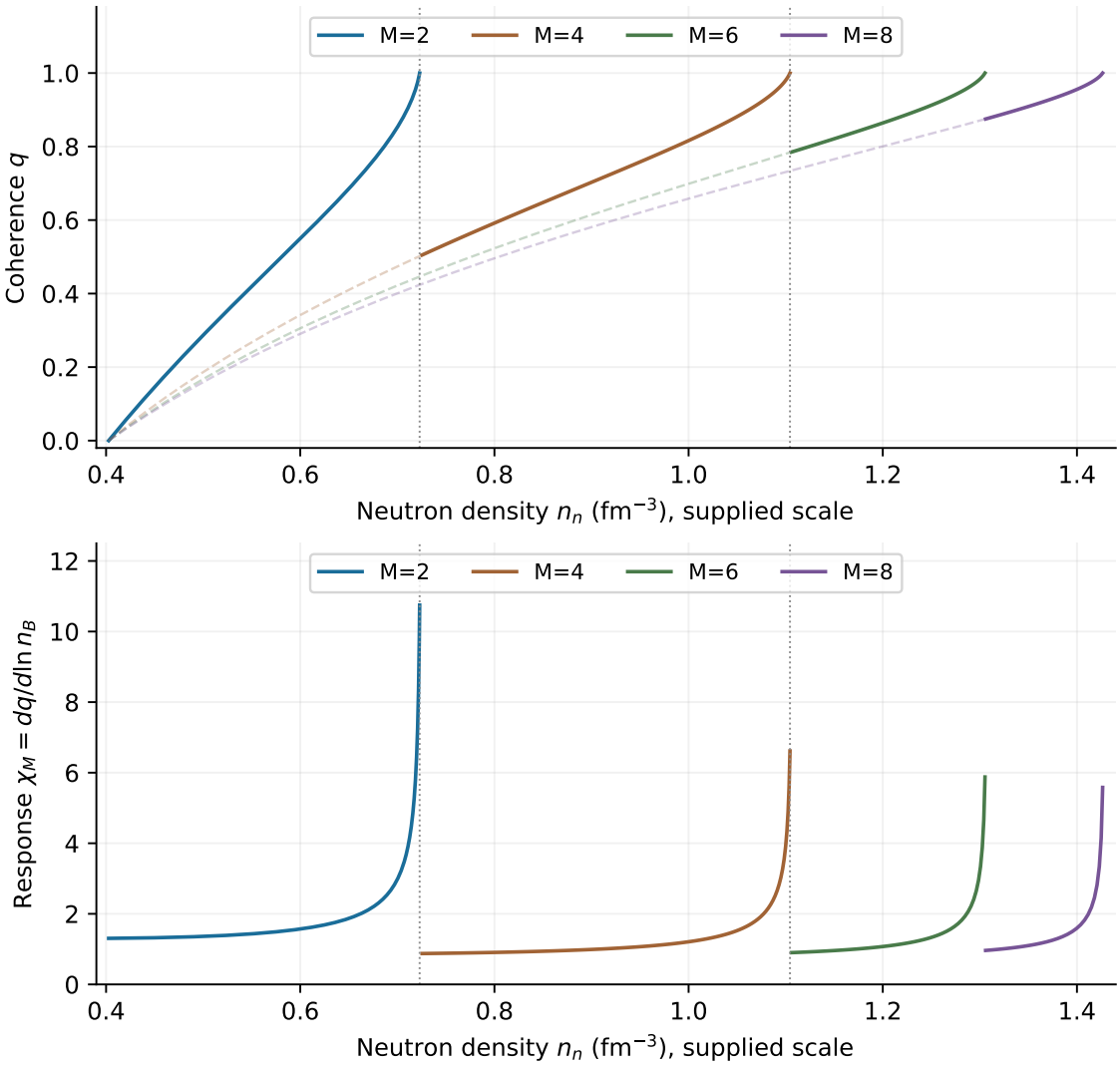

Figure 1: Prescribed collective branches and their response to compression. Solid portions show the saturation-and-minimum-M prescription; lighter continuations exhibit overlapping mathematical representations. The lower panel displays $\chi_M = -D/(3D_q)$, the geometric coefficient that enters the constitutive pressure. Vertical changes in the selected coefficient occur at geometrically continuous recruitment boundaries.

7 What the QMU conductance ledger supplies

The native identities retained from the construction are

$$e_{\mathrm{emax}}{}^2 = \mathrm{angm}\,\mathrm{cond}, \qquad \mathrm{cond} = \frac{1}{\mathrm{mflx}} = \frac{\mathrm{curl}}{c} = \frac{c}{A_u} = \frac{c}{\mathrm{rmfd}}. \tag{30}$$

They concern invariant QMU units and are consistent with $A_u\,\mathrm{curl} = c^2$ Thomson [2025c,a]. They do not determine a strain energy. The proposed local boundary assignment

$$C_A = D_{\mathrm{cell}}\,\mathrm{cond}, \qquad \frac{\mathrm{mflx}_A}{\mathrm{mflx}} = D_{\mathrm{cell}}^{-1} \tag{31}$$

is a constitutive identification, not a consequence of dimensional algebra. Its reciprocal relations can be maintained as definitions of local coefficients without varying the fundamental units themselves.

Even if Eq. (31) is adopted exactly, conductance and reciprocal magnetic flux are insufficient to give the work done under compression. That work requires a generalized force, an energy functional, or an action. The phase-chain construction supplies a possible organization of correlations; it does not provide the mechanical energy normalization of those correlations.

8 Source-completion theorem

8.1 Conserved density and constitutive assumptions

Neutron fraction can change in reacting matter. We therefore use conserved baryon density n_B, neutron fraction $Y_n > 0$, and

$$n_n = Y_n n_B, \qquad \nu_B = n_B \lambda_C^3. \tag{32}$$

The following result concerns a fixed-Y_n compression, or the frozen-composition part of a fuller reacting model. It assumes a reversible local equilibrium description, negligible resolved gradients, and isotropic stress after coarse graining. A single phase chain need not have isotropic stress; orientation averaging or a microscopic isotropic state must justify that assumption. An anisotropic completion instead requires additional strain variables and directional stresses.

Use the native energy and pressure-density units

$$E_q = \mathrm{angm} F_q = m_e \lambda_C^2 F_q^2, \qquad P_q = \frac{E_q}{\lambda_C^3}. \tag{33}$$

For the conventional bridge, $E_q = m_e c^2$. Let the proposed interaction contribution to energy density be

$$\varepsilon_A = E_q n_B u(\nu_B, Y_n, M, q), \tag{34}$$

where u is a dimensionless energy per baryon that a microscopic APM calculation must supply. This is the missing constitutive function, not a fitted expression chosen in this paper. Any baseline energy must exclude the same interaction contribution to avoid double counting an effect already included in an EOS.

Theorem 8.1 (Constrained source completion)**.** *On a differentiable fixed-M registration segment with $D_q \neq 0$, at fixed Y_n, define*

$$\chi_M(q) = -\frac{D(M,q)}{3D_q(M,q)}. \tag{35}$$

Then

$$\boxed{\frac{dq}{d\ln n_B} = \chi_M(q).} \tag{36}$$

If Eq. (16) is a mechanically enforced equilibrium constraint and its reaction work is included, the reduced energy $\bar{u}_M(\nu_B, Y_n) = u(\nu_B, Y_n, M, q_M)$ has constitutive pressure

$$\boxed{\frac{p_A}{E_q n_B} = \nu_B \frac{d\bar{u}_M}{d\nu_B} = \nu_B u_{\nu_B} + \chi_M u_q.} \tag{37}$$

Thus specifying u supplies both a rest-frame energy density and the associated isotropic constrained pressure, rather than an arbitrary scalar source multiplier.

Proof. At fixed Y_n, Eq. (1) gives $dD_{\rm cell}/d\ln n_B = -D_{\rm cell}/3$. Differentiating the registration proves Eq. (36). The zero-temperature fixed-composition first law gives $p_A = n_B\, d\varepsilon_A/dn_B - \varepsilon_A$ for the reduced energy contribution Brown [1993]. Substitution of Eq. (34) and the chain rule give Eq. (37). This operation varies the constrained state, so its work includes the reaction needed to maintain the registration. □

The pressure formula is not valid merely because an unconstrained internal coordinate happens to follow the same curve. If q is an independent dynamical variable, its generalized work, relaxation equation, and entropy production must instead be retained. Eliminating it requires an actual equilibrium or constraint principle. At a point where $D_q = 0$, this density-to-q parametrization fails and the theorem makes no regularity claim.

In native units the completion is

$$\frac{\varepsilon_A}{P_q} = \nu_B \bar{u}_M, \qquad \frac{p_A}{P_q} = \nu_B(\nu_B u_{\nu_B} + \chi_M u_q). \tag{38}$$

If u depends only on M and q, $p_A/(E_q n_B) = \chi_M u_q$. On a decreasing branch $\chi_M > 0$, so positive pressure in this sector requires increasing energy with increasing coherence. This is a constraint on a proposed microscopic energy, not a derivation of that energy.

8.2 A variational check of the constraint work

At fixed M, Y_n, write a local constrained energy density

$$\mathcal{E} = E_q n_B u + Lambda\left[D(M,q) - (Y_n n_B V_{n0})^{-1/3}\right]. \tag{39}$$

Stationarity in q gives $\Lambda = -E_q n_B u_q/D_q$. The contribution of the constraint to $n_B\partial\mathcal{E}/\partial n_B - \mathcal{E}$ on its constraint surface is $\Lambda D/3$. Substitution recovers exactly the $E_q n_B \chi_M u_q$ term in Eq. (37). This local check does not replace a full number-conserving fluid action Brown [1993], but shows which mechanical reaction would be omitted by taking a fixed-q pressure derivative.

For variable composition,

$$\frac{dq}{d\ln n_B} = \chi_M \left(1 + \frac{d\ln Y_n}{d\ln n_B}\right). \tag{40}$$

The composition dependence and chemical reactions must therefore be supplied by the total matter theory. One cannot infer the full stellar pressure from a neutron-density path alone.

9 What the geometry cannot identify

Theorem 9.1 (Geometric source nonuniqueness)**.** *The winding condition, Fejér/Toeplitz registration, QMU unit identities, and boundary assignments in Eq.* (31) *do not determine the constitutive function u, its energy normalization, or a unique stress–energy source.*

Proof. None of those relations contains u. Keeping their states fixed while replacing any proposed energy function by a different smooth energy function leaves every geometric relation unchanged, but changes Eq. (34) and generally Eq. (37). Even an imposed zero-density reference and basic stability do not remove this freedom: the family $u_a = a\nu_B$, $a > 0$, has $\varepsilon_A = p_A = E_q a \lambda_C^3 n_B^2$ while preserving the same geometry. Different a give different sources. These functions are counterexamples establishing nonuniqueness, not proposed APM interaction laws. □

For example, adding that illustrative sector to a positive rest-energy term $\varepsilon_0 = m_0 c^2 n_B$ gives

$$\frac{c_s^2}{c^2} = \frac{2a m_e \lambda_C^3 n_B}{m_0 + 2a m_e \lambda_C^3 n_B} < 1. \tag{41}$$

Thus the freedom is not removed just by requiring a positive, subluminal illustrative EOS. Nor does knowing the empirical neutron rest mass determine the density-dependent interaction energy. A neutron-specific microscopic calculation is still required.

The branch ambiguity in Eq. (19) is a second, distinct underdetermination. A source theory must identify both the energy on each admissible branch and the selection or recruitment mechanism. Calling the geometric family free of EOS-fitted coefficients does not remove these model choices.

10 Recruitment conditions imposed by energy and stress

Let a prescribed continuous-density transition occur at $n_{B,j}$, with fixed composition, old branch $(M, 1)$ and new branch $(M+2, q_{\text{entry}})$. Define

$$P_M = \nu_B u_{\nu_B} + \chi_M u_q. \tag{42}$$

Take the baseline energy to be branch independent, and include all branch-dependent recruitment costs in u. If there is no latent energy, surface work, or external reservoir at the transition, continuous energy and pressure require

$$\boxed{u_- = u_+, \qquad P_- = P_+.} \tag{43}$$

At the same n_B, these conditions also match the sector's chemical-potential contribution $E_q(u + P)$. They are conditions for this particular reversible continuous-density interpretation, not universal

conditions for every first-order phase transition. A phase-coexistence construction can instead involve different densities, chemical equilibrium, and interface contributions.

For an energy $u_M(q)$ without explicit density dependence, Eq. (43) becomes

$$u_M(1) = u_{M+2}(q_{\text{entry}}), \quad \chi_M(1)u'_M(1) = \chi_{M+2}(q_{\text{entry}})u'_{M+2}(q_{\text{entry}}). \tag{44}$$

The first transition has

$$\chi_2(1) = 10.74768448, \qquad \chi_4(0.5018956394) = 0.87390083. \tag{45}$$

Consequently, when the old energy slope is nonzero, the new slope must be approximately 12.2985 times the old slope to preserve pressure in this restricted $u_M(q)$ completion. The exact ratio is reported by the reproduction script. Continuity of D, conductance, and reciprocal flux does not enforce either condition in Eq. (44).

If energy is discontinuous at fixed density, the local difference is

$$\Delta\varepsilon_A = E_q n_{B,j}(u_+ - u_-). \tag{46}$$

A physical account must identify where that energy goes or comes from. Likewise, a pressure discontinuity requires a dynamical or interface treatment. The geometric branch change alone supplies neither.

On a smooth branch the total energy per baryon, including baseline matter, may be written $E_q\bar{f}(\nu_B)$ at fixed composition. Positive chemical response and a causal frozen-composition sound speed require

$$\bar{f} + \nu_B\bar{f}' > 0, \qquad 0 \le \frac{c_s^2}{c^2} = \frac{2\nu_B\bar{f}' + \nu_B^2\bar{f}''}{\bar{f} + \nu_B\bar{f}'} \le 1. \tag{47}$$

These constraints apply to the total EOS, not to an isolated interaction sector irrespective of its baseline. They also require at least two derivatives of the reduced constitutive energy. Global stability and branch selection require additional energy comparisons; a local sound-speed condition is not sufficient.

11 Connection to the gravitational source

The energy and stress obtained above are the quantities needed for a gravity calculation. The conversion to a mass-density contribution in the fluid rest frame is $\rho_A = \varepsilon_A/c^2$, not a new neutron mass formula. In the QMU normalization of AMC,

$$\widehat{\rho}_A^{\text{com}} = \frac{\rho_A\lambda_C^3}{m_a} = \frac{m_e}{m_a}\nu_B\bar{u}_M, \qquad \widehat{p}_A = \frac{p_A\lambda_C^3}{m_a c^2} = \frac{m_e}{m_a}\nu_B P_M. \tag{48}$$

No identification of m_e/m_a with an Aether fine-structure parameter is used. The primordial or empirically calibrated scale m_a fixes the normalization; it does not fix u.

For a specified static spherical trial profile in the GR correspondence, the contribution to the enclosed mass equation is

$$\frac{d\,\delta m_A}{dr} = 4\pi r^2\frac{\varepsilon_A}{c^2}. \tag{49}$$

With $\rho = r/\lambda_C$ and $\delta\mu_A = \delta m_A/m_a$, this is

$$\boxed{\frac{d\,\delta\mu_A}{d\rho} = 4\pi\rho^2 \frac{m_e}{m_a}\nu_B \bar{u}_M.} \tag{50}$$

The contribution to the radial compactness bookkeeping is then $\delta\vartheta_A = \delta\mu_A/\rho$ and $\delta\epsilon_A = 2\delta\vartheta_A$. This is not an assertion that the stationary unit-lapse PG ansatz is a positive-pressure stellar interior. In a self-consistent star, changed pressure also changes the density profile and all other matter contributions; integrating Eq. (49) on an unchanged profile is only a trial-profile source diagnostic.

The standard spherical mass equation uses rest-frame energy density with areal radius; its $4\pi r^2 dr$ measure is not the proper-volume baryon-number measure. Pressure enters stellar equilibrium separately Oppenheimer and Volkoff [1939]. In particular, replacing the mass source by $\rho_A + 3p_A/c^2$ would mix distinct gravitational source constructions. A lapse, stresses, and observer frame must be specified consistently.

For an isotropic comoving sector observed by slice-normal observers with relative Lorentz factor W, its energy projection is instead

$$\mathcal{E}_A^{\text{normal}} = (\varepsilon_A + p_A)W^2 - p_A. \tag{51}$$

This is the relevant type of projection for a Hamiltonian constraint Brown [1993]. It need not equal the rest-frame contribution in Eq. (48). A physically completed source functional therefore requires the constitutive energy, branch, composition, and observer relation, in addition to neutron density.

11.1 Neutron-composition response of the source

At fixed n_B on a smooth fixed-M branch, the same constraint gives

$$\frac{\partial q}{\partial Y_n} = \frac{\chi_M}{Y_n}. \tag{52}$$

Consequently the neutron-fraction dependence of the comoving source is

$$\boxed{\left.\frac{\partial \widehat{\rho}_A^{\text{com}}}{\partial Y_n}\right|_{\nu_B,M} = \frac{m_e}{m_a}\nu_B\left(u_{Y_n} + \frac{\chi_M}{Y_n}u_q\right).} \tag{53}$$

This separates explicit neutron-specific energy dependence from the dependence mediated by collective compression. For a restricted energy $u_M(q)$ with no additional explicit density or composition dependence, the pressure and composition responses must satisfy the exact branchwise identity

$$\boxed{Y_n \left.\frac{\partial \varepsilon_A}{\partial Y_n}\right|_{n_B,M} = p_A,} \qquad Y_n \left.\frac{\partial \rho_A^{\text{com}}}{\partial Y_n}\right|_{n_B,M} = \frac{p_A}{c^2}. \tag{54}$$

More generally, their difference is

$$p_A - Y_n \left.\frac{\partial \varepsilon_A}{\partial Y_n}\right|_{n_B,M} = E_q n_B(\nu_B u_{\nu_B} - Y_n u_{Y_n}). \tag{55}$$

These are local source-consistency tests for a future microscopic energy calculation. The fixed-baryon-density derivative changes composition; it is not a prediction of the free neutron mass or of

the captured electron–proton mass difference. Charged components and reaction equilibrium must be included before interpreting it as a complete stellar composition response.

In the weak-field, negligible-pressure limit, the conventional bridge is the contribution $\delta\rho_A = \varepsilon_A/c^2$ to Poisson's source. This paper does not modify the measured gravitational coupling or the Schwarzschild exterior path law. It supplies the conditions under which a future independently derived neutron–Aether interaction energy can be turned into a source and tested, without using a gravity fit to choose that energy.

12 Scientific tests and the next microscopic calculation

The geometric family makes conditional statements about admissible cell coordinates and their compression response. A decisive physical calculation must do more than invert the registration. It must derive a local interaction energy or action from neutron/Aether structure, explain or replace the assumed Toeplitz correlations and two-seat organization, and determine the energetic cost of recruitment. Given such a calculation, the present results specify the following checks:

1. Evaluate u and its density and coherence derivatives independently of neutron-star gravitational fits. Equation (37) then determines the constrained pressure contribution.
2. Compare energies on overlapping admissible branches. Test whether the proposed saturation rule follows from minimization or from an explicit nonequilibrium recruitment dynamics.
3. Check energy and pressure matching or supply the latent-energy, transport, and interface terms at each transition. The response factors in Eq. (45) make the first check quantitative.
4. Combine the interaction with a consistently defined baseline EOS, enforce the relevant composition and stability conditions, and solve the stellar stress and metric equations together.
5. Predict a mass–radius, tidal, or other observable before independent comparison. Geometric compatibility with a supplied SLY4 density is not that comparison.

The geometry alone does not predict an observable transition at 0.722973 or 1.104423 fm^{-3}, an additional photon-path parameter, or an excess neutron gravitational mass. Those statements would require the missing physical completion. The prescribed density scales and transfer coefficient are inputs to testing that completion rather than substitutes for it.

13 Conclusion

Collective Aether-cell coherence supplies a mathematically explicit extension of a restricted single-unit registration. Its strongest contribution to the neutron-to-gravity problem is a source-completion constraint: once a local constrained interaction energy is independently known, the geometry fixes how its coherence derivative enters pressure. In native units,

$$\frac{\varepsilon_A}{P_q} = \nu_B \bar{u}_M, \qquad \frac{p_A}{P_q} = \nu_B(\nu_B u_{\nu_B} + \chi_M u_q), \qquad \chi_M = -\frac{D}{3D_q}. \tag{56}$$

The phase-chain construction provides an explicit local statistical realization of the assumed correlations. The asymptotic proof fixes the geometric supremum and its leading approach. Branch overlap and source nonuniqueness show why neither density registration nor conductance identities

alone determine a physical source. Recruitment additionally requires energetic selection and thermodynamic matching, whose first response-factor jump is now quantified.

The additional composition relation, Eq. (53), specifies how the same constrained energy would enter a neutron-fraction-dependent source. In the coherence-only reduction it yields $Y_n \partial \varepsilon_A / \partial Y_n = p_A$, providing a direct consistency relation between composition response and pressure. These results delimit a concrete microscopic target: calculate a neutron–Aether interaction energy and recruitment cost, then use the derived response and matching conditions to obtain a consistent stress–energy contribution. That is the remaining step between a collective geometric representation and a neutron-specific gravitational source law.

A Numerical reproduction and provenance

The package includes `scripts/reproduce.py`, versioned numerical dependencies, generated figures, branch tables, response coefficients, and a machine-readable summary. The script evaluates Eqs. (9) and (35), solves the stated branch-entry constraints, checks the overlapping representations, verifies the phase-chain matrix identity, and checks the source derivative by finite differences of a declared mathematical test function. That test function is used solely to verify the chain rule and is not proposed as an APM energy law.

The boundary-layer integral is computed by period-wise quadrature of a rationalized excess integrand. Its large-R tail uses

$$\int_R^\infty \left[\sqrt{1 + 4\sin^4 y/y^2} - 1\right] dy = \frac{3}{4R} - C_2(R) + \frac{1}{4}C_4(R) - \frac{35}{192R^3} + O(R^{-4}), \tag{57}$$

where $C_a(R) = \cos(aR)/R - a[\pi/2 - \mathrm{Si}(aR)]$. Agreement at several period-aligned cutoffs and a separate high-M calculation check the stated numerical precision; this is a numerical check rather than a certified interval bound. The asymptotic scaling itself follows from the dominated-convergence proof in Sec. 6.

The radius and SLY4 density are supplied inputs retained for continuity with the earlier work. Their upstream microscopic and stellar calculations are not reproduced. No raw EOS reconstruction, neutron-radius derivation, observed coherence data, or microscopic interaction energy is supplied or fabricated. The existing DOI is retained as the work identifier; the version-specific identifier must follow the actual deposition.

Acknowledgments

The Quantum AetherDynamics Institute develops the Aether Physics Model and Quantum Measurement Units Thomson [2025b]. Publications are archived in the AetherPhysics Zenodo community.

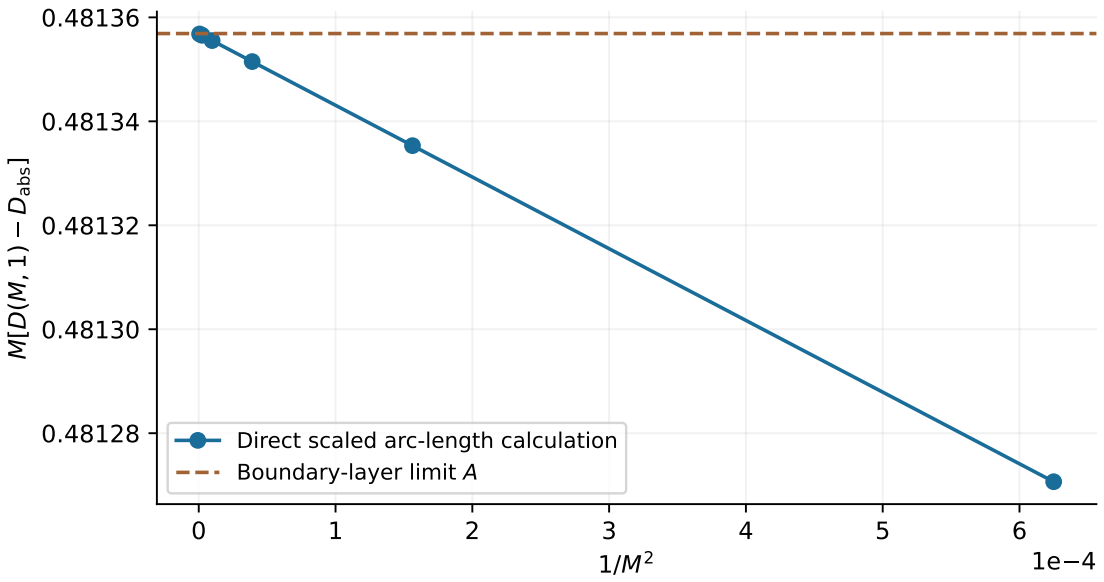

Figure 2: Independent high-M verification of the corrected boundary-layer coefficient. The horizontal limit is evaluated from the improper integral, not fitted to the finite-M sequence. Plotting against $1/M^2$ is a numerical diagnostic, not an additional asymptotic theorem.

References

J. David Brown. Action functionals for relativistic perfect fluids. *Classical and Quantum Gravity*, 10(8): 1579–1606, 1993. doi: 10.1088/0264-9381/10/8/017.

J. R. Oppenheimer and G. M. Volkoff. On Massive Neutron Cores. *Physical Review*, 55:374–381, 1939. doi: 10.1103/PhysRev.55.374.

David W. Thomson, III. The Charge Conversion Factor in the Aether Physics Model: From Singular to Distributed Charge, with Rules, Exceptions, and Benchmarks, 2025a. URL https://doi.org/10.5281/zenodo.17451188.

David W. Thomson, III. Quantum AetherDynamics Institute (QADI): Community DOI Overview and Citation Guide. Zenodo, 2025b. URL https://doi.org/10.5281/zenodo.17479314.

David W. Thomson, III. Reference Tables for Quantum Measurement Unit (QMU) Conversions: CGS and MKS Systems, 2025c. URL https://doi.org/10.5281/zenodo.17683574.

David W. Thomson, III. Aether Metric Coordinates: Neutron-Induced Length-Density Strain and Photon-Path Curvature in Compact Objects, 2026. URL https://doi.org/10.5281/zenodo.22087711. Companion manuscript revision, version 1.4, October 17, 2026.